PHILOSOPHICAL TRANSACTIONS OF THE ROYAL SOCIETY A MATHEMATICAL, PHYSICAL & ENGINEERING SCIENCES

Phase Mappings from Diffusion-Coupled Excitable Chemical Systems

Juraj Kosek, Igor Schreiber and Milos Marek

Phil. Trans. R. Soc. Lond. A 1994 **347**, 643-660
doi: 10.1098/rsta.1994.0072

Phase mappings from diffusion-coupled excitable chemical systems†

By Juraj Kosek, Igor Schreiber and Miloš Marek

Department of Chemical Engineering, Prague Institute of Chemical Technology, 166 28 Prague 6, Technická 5, Czech Republic

Dynamics of a cascade of two diffusion-coupled excitable units periodically perturbed by pulses applied to the first cell is examined. Firing sequences experimentally found in a chemical system constituted by two coupled stirred cells with the Belousov–Zhabotinskii (BZ) reaction are modelled on two levels. A phase mapping of an abstract piecewise linear excitable two-cell system is derived and its dynamics examined in detail. The functional form of this map combined with local excitation dynamics extracted from a realistic model of the BZ kinetics is used to formulate a semi-empirical model directly applicable to the experimental BZ system. The frequency of firings in the second cell can be either equal to that in the first cell – a complete propagation of the excitation, or smaller – a propagation failure. Complex patterns of transitions between the two dynamic modes found in experiments are well predicted by the semi-empirical model and, surprisingly, by the abstract model as well, pointing to a generic nature of the patterns.

1. Introduction

Excitable chemically reacting liquid ionic systems and excitable biological systems, such as chemical or electric synapses, specific receptors, neurons, neural networks, various excitable tissues (e.g. heart), etc., share a number of common properties. On a macroscopic level of description excitability is associated with rapid changes of temporal and spatiotemporal patterns of concentrations and fluxes of reacting and/or transported (via diffusion, ionic migration or convection) chemical species in response to a stimulation by an external perturbation of concentration, temperature, light, etc. Particular mechanisms of excitation in biological systems are mutually coupled in a complex and often still not identified way. Hence relatively simpler chemical systems operated under well-controlled conditions, for instance a continuous flow-through reaction cell (CSTR) or a network of coupled CSTRs, can serve as a tool for testing different ways of description of excitable systems.

A widely used technique for studying the phase-resetting of biological clocks by an external stimulus is based on the measurements of phase shifts of oscillations caused by perturbing the system at various phases of the clock; see, for example,

† This paper was produced from the authors' disk by using the TEX typesetting system.

Phil. Trans. R. Soc. Lond. A (1994) **347**, 643–660
Printed in Great Britain

a recent study of circadian rhythms in prokaryotes (Kondo *et al.* 1993). The variation of the phase shift with the phase of the perturbation is represented by a one-dimensional mapping – *the phase response curve* (PRC) (Winfree 1977; Glass & Mackey 1988; Glass *et al.* 1991).

Such a mapping was constructed from measurements of a chemical oscillatory system – the Belousov–Zhabotinskii (BZ) reaction – run in a CSTR (Dolník *et al.* 1986). Repeated iterations of a map simply related to the PRC provide an excellent way of predicting the dynamics, periodic as well as aperiodic, observed in the CSTR periodically perturbed by pulse additions of a reactant (Dolník *et al.* 1986; Marek & Schreiber 1991, ch. 5). The dynamic response to single as well as repeated pulse stimulations of the excitable BZ reaction was also a subject of our previous work (Dolník *et al.* 1989; Finkeová *et al.* 1990). A one-dimensional map analogous to the PRC, *the phase excitation curve* (PEC), was constructed from the responses to multiple stimulations and used in predicting the dynamics of the periodically perturbed excitable BZ reaction in the same fashion as the PRC in the case of the oscillatory BZ system (Dolník & Marek 1991, Dolník *et al.* 1992). The experimental technique for the construction of the PEC was tested on several kinetic schemes for the BZ and other chemical systems and used for the construction of a resonance (or excitation) diagram – the plot of a firing number against the period and/or the amplitude of the perturbation. The firing number measures the average number of the events of excitation within one forcing period (Alexander *et al.* 1990).

The outlined methods are equally applicable to biochemical and biological systems. There is a striking analogy between complex biological and simple chemical systems manifested by a similar structure of the excitation diagrams of the BZ reaction and those reported for periodically stimulated giant axons of squid (Takahashi *et al.* 1990; Dolník & Marek 1991).

Excitatory and oscillatory units in biological systems (receptors, neurons) are frequently coupled, locally or globally, chemically or electrically. Information transmission and coding in such networks is tied with the properties of outcoming sequences of interspike intervals (firing patterns). Specific cells can be activated by a particular stimulus and the resulting firing pattern may serve a physiological function, e.g. to encode visual images of objects or to provide a mechanism of short term memory or learning (Tanaka 1992; Fujita *et al.* 1992; Hammer 1993). Coupled chemical oscillators and excitators have been the subject of several recent experimental and computer-assisted studies; see Schreiber & Marek (1993), Yoshimoto *et al.* (1993) and Zeyer *et al.* (1993) for recent reviews. Formally derived models based on cellular automata and coupled map lattices have been primarily used for studies of cooperative dynamics in coupled systems (Kaneko 1990; Chawanya *et al.* 1993). A closely related problem of modelling waves and other dynamical phenomena in excitable media with continuous space is also of considerable interest (Holden *et al.* 1991; Barkley 1991).

Several theoretical works use a phase model that describes a single oscillatory or excitable unit by (Kuramoto 1991)

$$\mathrm{d}\phi/\mathrm{d}t = v(\phi), \tag{1.1}$$

where the phase ϕ is a cyclic variable. The equation corresponds to excitable dynamics if the vector field v contains a stable stationary point and to oscillatory dynamics if there is no ϕ such that $v(\phi) = 0$. Development of methods for

PHILOSOPHICAL TRANSACTIONS OF THE ROYAL SOCIETY A MATHEMATICAL, PHYSICAL & ENGINEERING SCIENCES

the construction of a phase model having the form of (1.1) and consistent with experimental data represents an important step in efforts aimed at modelling of networks of biological excitable elements.

In this paper we shall describe a specific mapping that reproduces excitation diagrams constructed from the experiments with two coupled chemical cells with the BZ reaction in the excitable mode externally driven by periodic pulses introduced into one of the cells. We shall be particularly interested in the description of the *propagation failure* dynamics. This phenomenon occurs when the event of excitation fails to propagate into the second cell each time a pulse elicits an excitation in the first cell; the propagation failure can be controlled by external constraints (Kosek & Marek 1993). A similar behaviour, selective elimination of synapses, has been described in formal enzymatic neuron models (Okamoto 1992).

In § 2 a piecewise linear phase model that captures essential features of a general excitable system is introduced and the dynamics of a phase excitation map derived for two coupled excitable units is examined. Section 3 reviews our recent experimental work followed by a procedure that combines the detailed knowledge of the dynamics of the piecewise linear phase model of § 2 with a map extracted from a realistic model of the BZ reaction to produce a BZ phase excitation map whose dynamics is compared to experimental findings.

2. Phase model

A linear N-array of identical oscillatory or excitable units coupled linearly (i.e. diffusion-like) may be described by

$$\mathrm{d}\boldsymbol{x}_i/\mathrm{d}t = \boldsymbol{f}(\boldsymbol{x}_i) + d(\boldsymbol{x}_{i+1} - 2\boldsymbol{x}_i + \boldsymbol{x}_{i-1}), \quad i = 1, \ldots, N, \quad \boldsymbol{x}_i \in R^n, \tag{2.1}$$

supplemented by a set of boundary conditions, for example no flux at the ends, $\boldsymbol{x}_0 = \boldsymbol{x}_1$, $\boldsymbol{x}_{N+1} = \boldsymbol{x}_N$. The local dynamics of each unit is given by the function $\boldsymbol{f}(\boldsymbol{x})$, d is the transport coefficient. A pulse perturbation of the unit 1 may cause its firing and the excitation can be propagated through the array. If the pulse is applied periodically, the conditions for propagation will depend on the input frequency, the amplitude of the pulse and the transport coefficient.

The reduction of (2.1) to phase equations assumes that there is a one-dimensional set Λ in R^n such that the local dynamics in each unit is, after a rapid transient, confined to it; Λ is a *limit cycle* for an oscillator and an *excitable cycle* for an excitator. Whereas the limit cycle is a single closed trajectory γ , the excitable cycle is formed by two trajectories γ_1, γ_2, both approaching a stable stationary state $\boldsymbol{x}_\mathrm{s}$ from opposite directions as $t \to \infty$. There are two basic situations in the state space corresponding to two basic modes of excitability: (a) there is an additional (saddle) stationary point such that γ_1 and γ_2 approach it as $t \to -\infty$, (b) there is no such point; γ_1 and γ_2 come close to each other in reverse time, eventually creating a narrow gap, but never join up. The case (a) uniquely defines the excitable cycle Λ, whereas the case (b) does not; an additional assumption of strong stability of Λ has to be made. In both cases, there exists a slow manifold, the *threshold set* (Alexander *et al.* 1990), separating two kinds of trajectories that correspond to excitation events and no excitations. When perturbed at or near to $\boldsymbol{x}_\mathrm{s}$ so that the state of the system gets beyond the threshold set, the system undergoes an excitation event; otherwise no excitation

occurs. The threshold set may be a surface or a layer of finite thickness, locally separating the state space R^n.

Once identified, Λ can be parametrized by a coordinate ϕ called the phase. A scaled time may be a good choice for an oscillator but a different parametrization, such as the arclength along Λ, is more convenient for an excitator due to the presence of stationary state(s) in Λ.

We want a simple description that would comprise the two cases of excitability. This is achieved by selecting two points, $P_1 \in \gamma_1$ and $P_2 \in \gamma_2$, such that their distance is small compared to the size of the excitable cycle, neglecting the gap between them and making P_1 identical to P_2 . In fact, the gap is filled with the threshold set whose width is, by virtue of approximation, reduced to zero. We set the phase $\phi = 0$ at P_1 and $\phi = 1$ at P_2. By this procedure we get the advantage of having a cyclic phase space in exchange for the inconvenience of having a discontinuity in the velocity function on the phase circle.

A phase model of an excitable unit obeys (1.1); the velocity function $v(\phi)$ is determined by the dynamics of (2.1) on Λ for N=1. The simplest form of v is $v = a - \phi$ with ϕ restricted to a circle S^1 of length 1, $0 \leqslant \phi < 1$. Let us assume that a perturbation will shift ϕ instantaneously by an amplitude A in the positive direction (given by increasing ϕ) along the cycle. Furthermore, we locate the stationary point $\phi_s = a$ just below the threshold at $\phi = 0$ so that $\phi_s + \varepsilon = 0$ (mod 1), $0 < \varepsilon \ll 1$. Clearly, a moderate but superthreshold perturbation $A \geqslant \varepsilon$ of the system at ϕ_s will cause ϕ to jump over the threshold and then increase until ϕ_s is reached again (an excitation event); a subthreshold perturbation will cause ϕ to approach the steady state in the negative direction (no excitation).

The simplest phase system that admits the propagation failure phenomenon is the 2-array. The equations governing the dynamics under T-periodic forcing by a sequence of δ pulses of amplitude A are

$$\mathrm{d}\phi_1/\mathrm{d}t = a - \phi_1 + d(\phi_2 - \phi_1 - \varphi) + A\sum_i \delta(t - iT), \tag{2.2}$$

$$\mathrm{d}\phi_2/\mathrm{d}t = a - \phi_2 + d(\phi_1 - \phi_2 + \varphi). \tag{2.3}$$

The coupling makes it possible for trajectories to cross the threshold value $\phi_1 = \phi_2 = 0$ which leads to jumps and consequently to points of non-smoothness on trajectories. The coupling terms provide a different source of non-smoothness – diffusion on the circle must drive both phase variables to each other along the arc of shorter length. Hence a switch function φ is introduced to take care of this: (i) $\varphi = 0$ when $-\frac{1}{2} \leqslant \phi_1 - \phi_2 \leqslant \frac{1}{2}$; (ii) $\varphi = 1$ when $-1 < \phi_1 - \phi_2 < -\frac{1}{2}$; (iii) $\varphi = -1$ when $\frac{1}{2} < \phi_1 - \phi_2 < 1$.

The next step is to derive a Poincaré map associated with (2.2) and (2.3). A convenient means of doing so is stroboscopically taking samples just before the pulse. Starting with the initial state (ϕ_1, ϕ_2) and integrating the equations from $t = -\varepsilon$ to $t = \varepsilon$, ε being an arbitrarily small positive number, we obtain the pulse map P,

$$\phi_{1+} = \phi_1 + A \pmod 1, \tag{2.4}$$

$$\phi_{2+} = \phi_2. \tag{2.5}$$

Considering that between two consecutive δ pulses (2.2) and (2.3) are autonomous and piecewise linear the integration over a time interval of length τ between

two consecutive points of non-smoothness starting at (ϕ_{10}, ϕ_{20}) yields

$$\phi_1(\tau) = g(\phi_{10}; a, \tau) + D(d, \tau)(g(\phi_{20}; a, \tau) - g(\phi_{10}; a, \tau) - E(d, \tau)), \quad (2.6)$$

$$\phi_2(\tau) = g(\phi_{20}; a, \tau) + D(d, \tau)(g(\phi_{10}; a, \tau) - g(\phi_{20}; a, \tau) + E(d, \tau)), \quad (2.7)$$

where

$$g(\phi_{i0}; a, \tau) = a(1 - \mathrm{e}^{-\tau}) + \phi_{i0}\mathrm{e}^{-\tau}, \quad i = 1, 2,$$

$$D(d, \tau) = \tfrac{1}{2}(1 - \mathrm{e}^{-2d\tau}),$$

$$E(d, \tau) = 0 \qquad \text{if } -\tfrac{1}{2} < \phi_1(s) - \phi_2(s) < \tfrac{1}{2}, \quad \text{(i)}$$

$$= \frac{2d(1 - \mathrm{e}^{-(1+2d)\tau})}{(1 + 2d)(1 - \mathrm{e}^{-2d\tau})} \qquad \text{if } -1 < \phi_1(s) - \phi_2(s) < -\tfrac{1}{2}, \quad \text{(ii)}$$

$$= \frac{-2d(1 - \mathrm{e}^{-(1+2d)\tau})}{(1 + 2d)(1 - \mathrm{e}^{-2d\tau})} \qquad \text{if } \tfrac{1}{2} < \phi_1(s) - \phi_2(s) < 1, \quad \text{for } s \in [0, \tau]. \quad \text{(iii)}$$

Equations (2.6) and (2.7) reflect the functional form of (2.2) and (2.3); the function $g(\phi_{i0}; a, \tau)$ describes the relaxation portion of the dynamics of an isolated unit i since the coupling term disappears for vanishing d. The coupling terms are proportional to the phase difference of both units at the time τ corrected by the compensation term E that appears due to the condition for the diffusion on a circle; the integral transport coefficient D depends on τ as well as on d and ranges from 0 to $\frac{1}{2}$.

The time τ is determined implicitly by the instant of a jump in $\phi_1 - \phi_2$. Thus the Poincaré mapping Π taking a point $(\phi_{1,k}, \phi_{2,k})$ just before the kth pulse to $(\phi_{1,k+1}, \phi_{2,k+1})$ just before the $(k+1)$st pulse is made up by combining the pulse map P with a relaxation map F obtained by a product of three maps F^{τ_1}, F^{τ_2}, F^{τ_3} defined by (2.6) and (2.7) with the three different choices (i), (ii) and (iii) of E so that $T = \tau_1 + \tau_2 + \tau_3$. In general, the ordering of F^{τ_i}s varies in each iteration of Π depending on the order of occurrence of points of non-smoothness.

To understand the dynamics of the coupled system we first examine the dynamics of a periodically forced isolated unit. The mapping $g(\phi_+; a, T)$, where $\phi_+ = \phi + A \pmod 1$ is the pulse map, defines the Poincaré mapping of one cell T-periodically perturbed with δ pulses of amplitude A. The Poincaré mapping,

$$\Pi(\phi; a, T) = a(1 - \mathrm{e}^{-T}) + (\phi + A \pmod 1)\mathrm{e}^{-T} \quad (2.8)$$

is a piecewise linear function with a discontinuity at $\phi_r = 1 - A$. This is the phase of marginal refractoriness; the system fires only when perturbed at $\phi > \phi_r$. The slope of Π is less than 1 hence all orbits $\{\phi_k\}$ are stable. The dynamics of Π is well characterized by a rotation number (Alexander *et al.* 1990) expressing an average increment in ϕ per one iteration,

$$\rho = \lim_{k\to\infty} \frac{1}{k} \sum_{l=0}^{k-1} (A + \Pi(\phi_l; a, T) - \phi_{+,l}). \quad (2.9)$$

A firing number ν is an asymptotic average number of initiated excitation events per one forcing period. In one cell a superthreshold perturbation always initiates an excitation event. For each superthreshold perturbation $A + \Pi(\phi_l; a, T) - \phi_{+,l} = 1 + \Pi(\phi_l; a, T) - \phi_l$. Since $\sum_l \Pi(\phi_l; a, T) - \phi_l$ averages out, $\rho = \nu$. If $\nu = p/q$ (p,q coprime), then there is a phase-locked periodic régime with p excitation events

per q perturbations. From numerical calculations the firing number appears to be a non-decreasing stepwise function of T with many discontinuous jumps (a broken devil's staircase); ν vanishes at $T = 0$ and reaches its maximum value of 1 for T sufficiently large.

The dynamics of two coupled excitable units is more complex. A superthreshold perturbation of unit 1 does not necessarily imply an initiation of the excitation event because of a possible suppression by diffusion. None the less, the rotation numbers ρ_1, ρ_2 are defined in the same fashion as ρ for one cell and are equal to the firing numbers ν_1, ν_2 since ρ_is accommodate the diffusion suppressed (or induced) excitations. Typically, one can expect that ϕ_1 and ϕ_2 are near $\phi_s = a$ before the pulse and that ϕ_{1+} is slightly above the threshold. That is, the pulse changes the condition $-\frac{1}{2} \leqslant \phi_1 - \phi_2 \leqslant \frac{1}{2}$ to $-1 < \phi_1 - \phi_2 < -\frac{1}{2}$. Then two possible fates of ϕ_1 depend on whether diffusion drives ϕ_1 back *below* the threshold or not. If so, then no excitation occurs in the first cell and likewise the second cell cannot fire. If not, then the excitation event in the first cell occurs and the second cell may fire as well if diffusion drives ϕ_2 *above* the threshold. So the propagation failure is chiefly determined by the interaction of internal dynamics with diffusion during a time interval τ_2 when the condition $-1 \leqslant \phi_1 - \phi_2 \leqslant -\frac{1}{2}$ holds. The reverse situation, when $\frac{1}{2} < \phi_1 - \phi_2 < 1$ after the pulse, is much less frequent even though it may occur at high frequencies of the forcing. This implies that the Poincaré map is either $\Pi = F^{\tau_i} \circ P$, $i = 1, 2, 3$ or $\Pi = F^{\tau_1} \circ F^{\tau_2} \circ P$ or $\Pi = F^{\tau_1} \circ F^{\tau_3} \circ P$ depending on whether the condition (i), (ii) or (iii) holds after the pulse and whether there occurs a non-smooth point during the time interval T. An approximate but useful construction of Π relies on the assumption that an initial time interval τ_{in} during which the condition (ii) or (iii) switches to (i) is very short. Then $\mathrm{e}^{-\tau_{\text{in}}} \approx 1$ and $E \approx 1$ and

$$\Pi = F^{\tau_1} \circ F^{\tau_{\text{in}}} \circ P, \tag{2.10}$$

where

$$\left.\begin{aligned} F^{\tau_{\text{in}}} \circ P &= (\phi_1(\tau_{\text{in}}), \phi_2(\tau_{\text{in}})), \\ \phi_1(\tau_{\text{in}}) &= \phi_1 + A(1 - D_{\text{in}}) + D_{\text{in}}(\phi_2 - \phi_1), \\ \phi_2(\tau_{\text{in}}) &= \phi_2 + AD_{\text{in}} + D_{\text{in}}(\phi_1 - \phi_2), \\ D_{\text{in}} &= \tfrac{1}{2}(1 - \mathrm{e}^{-2d\tau_{\text{in}}}). \end{aligned}\right\} \tag{2.11}$$

The terms $\varepsilon_1 = A(1 - D_{\text{in}}) + D_{\text{in}}(\phi_2 - \phi_1)$ and $\varepsilon_2 = AD_{\text{in}} + D_{\text{in}}(\phi_1 - \phi_2)$ can be understood as effective amplitudes of a 'finite-time-jump' map $\hat{P} = F^{\tau_{\text{in}}} \circ P$. This allows us to define phases of marginal refractoriness in each cell, $\phi_{r1} = 1 - \varepsilon_1$ and $\phi_{r2} = 1 - \varepsilon_2$. The excitation event in the ith unit then occurs if $\phi_{i,k} > \phi_{ri}$. When checked numerically this criterion works quite well; it is not necessary to use it with the simple phase model (2.2) and (2.3) but it will be of importance in § 3.

Further analysis was carried out on a computer by using (2.6) and (2.7) to construct Π and calculating the vector of firing numbers (ν_1, ν_2). Clearly, the propagation failure phenomenon implies $\nu_1 \geqslant \nu_2$. The plot of ν_1, ν_2 against T is shown in figure 1. A characteristic feature of this excitation diagram, observed in our earlier experiments with the BZ reaction and computer simulations of full differential equations with a particular function $\boldsymbol{f}(\boldsymbol{x})$ corresponding to BZ kinetics, is seen here again. Namely, for each of the dominant steps with $\nu_1 = 1/q$, $q = 1, 2, 3$ in the first cell there is a whole staircase in the second one ranging

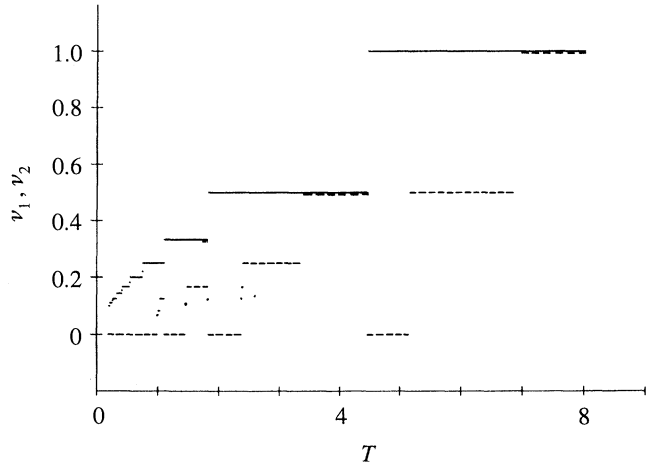

Figure 1. The plot of the firing vector (ν_1, ν_2) against T for the abstract phase map (2.4)–(2.7); $A = 0.035$, $d = 0.12$, $a = 0.98$; ——, first (externally driven) cell; - - -, second cell.

from $\nu_2 = 1$ to $\nu_2 = 0$. The dynamical régime is called a *complete propagation* when $\nu_1 = \nu_2 > 0$, a *partial propagation failure* when $\nu_1 > \nu_2 > 0$ and a *complete propagation failure* when $\nu_1 > \nu_2 = 0$. The complete propagation occurs in the right portion of each of the $1/q$-steps in the first cell and breaks down due to the propagation failure. The complete propagation is repeatedly restored as T is decreased until a limit is reached below which the staircase in the second cell does not have a full width (this first happens when $\nu_1 = \frac{1}{4}$ in the figure) and ultimately no excitation is propagated. The induced staircases in the second cell contain much less steps than the staircase in the first cell, in fact, there seem to be only a few resonances possible with large gaps in between. Figure 2 shows all major resonance regions (boundaries were calculated approximately) in the A–T parameter plane; each of the regions is distinguished by its firing vector (ν_1, ν_2) . The superthreshold area shows a hierarchical structure with a cross-similarity of the regions having the same ratio ν_2/ν_1. In general, complete propagation dominates for A slightly above the threshold, complete propagation failure becomes dominant as A is increased. A detailed structure of the boundaries is a subject of an ongoing study.

3. Excitable BZ system

(*a*) *Experiments*

The experiments with the BZ reaction in an excitable mode were carried out in two CSTRs coupled by a mutual mass exchange as shown in figure 3. The volume of each cell was $V = 70$ ml, the coupling strength was controlled by a movable teflon barrier. The height z of the barrier opening is proportional to the transport coefficient d (Stuchl & Marek 1982). Efficient stirrers (designed as Rushton turbines) with a controlled stirring rate set to 600 r.p.m. were used. Platinum and bromide ion selective electrodes were used to follow the course of the redox potential and the concentration of bromide ions in both cells. The conditions in both cells were kept the same: the inlet concentrations were $[Ce(SO_4)_2] = 0.006$ mol dm^{-3}, $[H_2SO_4] = 0.410$ mol dm^{-3}, $[CH_2(COOH)_2] = 0.1$ mol dm^{-3},

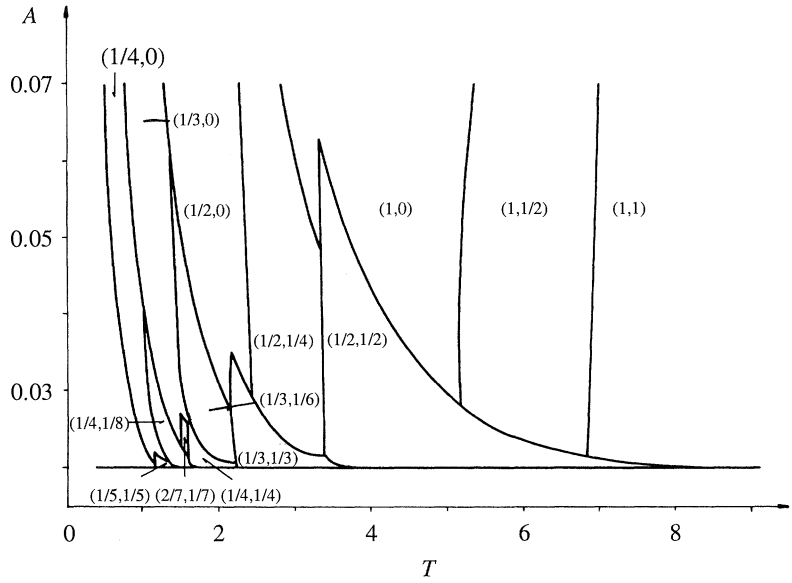

Figure 2. T–A excitation diagram for the abstract phase map (2.4)–(2.7); the value of the firing vector (ν_1, ν_2) defines a partition of the parameter plane into regions with particular dynamic modes; $d = 0.12$, $a = 0.98$.

$[KBr] = 0.01$ mol dm^{-3} and $[NaBrO_3] = 0.3$ mol dm^{-3}; the residence time was 31 min and temperature 20.0 °C. The cell R1 was perturbed by pulse addition(s) of a small volume (0.2–1.0 ml) of a solution of $AgNO_3$ (concentration 0.004–0.02 mol dm^{-3}) delivered within approximately 0.1–0.4 s. The added Ag^+ ions remove Br^- ions which control the autocatalytic reaction pathway. The amount of added Ag^+ ions divided by the volume V of the reactor represents an amplitude A of the perturbation. Three externally adjustable parameters were varied systematically: the transport coefficient d (through the height z), the amplitude A and the period T. Single pulse experiments can be treated as a special case of the periodically perturbed system with an infinitely large T.

(i) *Single pulse stimulation*

An excitation event in either cell was well indicated by the amplitudes of excursions of the bromide electrode potential; for given operating conditions the ratio (amplitude of an excitatory response)/(amplitude of a failed excitation) was never less than 3. There is a threshold value of A below which no excitation is generated. For superthreshold values of A there are three possible kinds of responses: (a) the first cell fires and after a time delay the second cell fires as well; it was found that the time delay is almost independent of A and only weakly dependent on d; (b) the propagation failure occurs; (c) no firing in any cell.

The occurrence of the three types of responses when the amplitude A and the coupling strength represented by z are varied is indicated in figure 4. The threshold value of the amplitude slightly increases with z and the propagation of the firing to the second cell requires a critical value of $z = z^*(A)$ to be exceeded; z^* increases with increasing A. Moreover, when A is varied for z fixed at a value within the range of z^*, the system passes through all three kinds of régimes: no firing for subthreshold amplitudes, both cells fire for an intermediate range of A ,

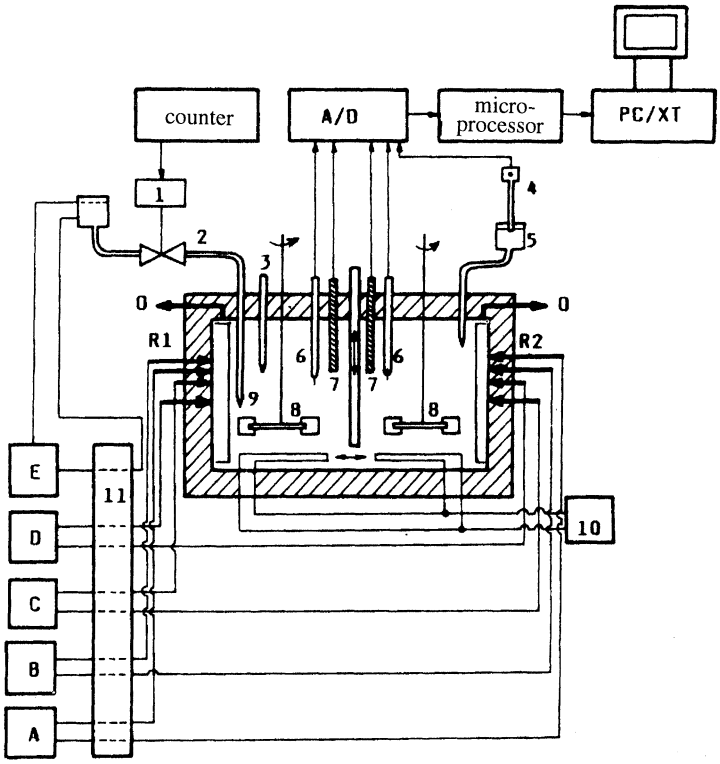

Figure 3. The experimental set up for two coupled CSTRs. (*a*) Solution of $Ce(SO_4)_2$ and H_2SO_4; (*b*) $CH_2(COOH)_2$; (*c*) KBr; (*d*) $NaBrO_3$; (*e*) $AgNO_3$. 1, valve control; 2, solenoid valve; 3, thermistor; 4, calomel electrode; 5, salt bridge; 6, platinum electrode; 7, bromide electrode; 8, stirrer; 9, dosing capillary; 10, thermostat; 11, dosing pumps.

propagation failure for A large enough. This means, somewhat counterintuitively, that an increase of the perturbation strength may cause a failure of the pulse propagation.

(ii) *Periodic pulse stimulations*

An 'experimental firing number' σ consistent with the definition of ν in §1 was used in earlier experiments with a periodically forced BZ reaction in a single CSTR (Dolník *et al.* 1989) to characterize the resonance régimes; σ is defined as P/Q where P is the number of firings and Q is the number of perturbations during an after-transient portion of the experiment. If the firing sequence can be decomposed into n blocks of length q with p firings in each block, i.e. $\sigma = np/nq$; p, q coprime, $n > 1$, there is a p/q *frequency-locked* or *synchronized* régime with p excitation events within q forcing cycles; taking into account an inevitable experimental noise, such a régime was usually considered periodic (and then called p/q *phase-locked*) but in general the period may be an integer multiple of q or there may be no period indicated. If n=1 then the dynamics is considered non-periodic without frequency-locking. Clearly, the use of σ in the non-periodic case must be approached with caution.

Here we use a firing vector (σ_1, σ_2) puting together two experimental firing

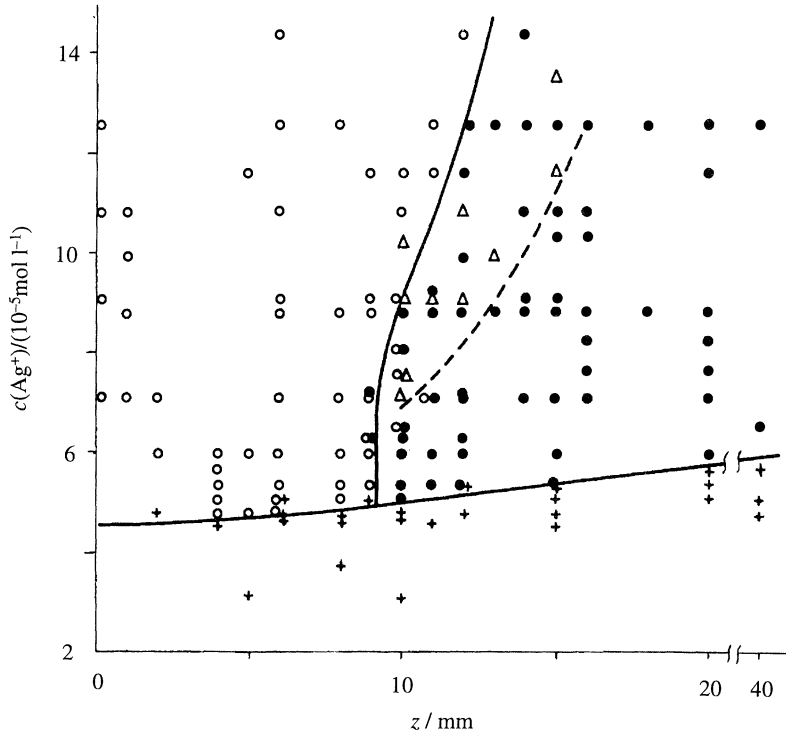

Figure 4. The type of the response to a single stimulation of varying amplitude $c(Ag^+) \equiv A$ for varying coupling strength z. +, No firing in either cell; ○, firing only in the externally perturbed cell; •, firing in both cells; △, firing in both cells but propagation failure is possible if forced periodically.

numbers associated with the dynamics in the two cells. Dynamical régimes observed in the experiments can be classified according to several criteria. One of them is the overall periodicity of the response. Another criterion is the occurrence of the propagation failure phenomenon. Yet another criterion is the mutual frequency-locking of the two cells. Here we choose the propagation failure criterion and find the following classes (assuming $\sigma_1 > 0$):

(a) The dynamics is called a *complete propagation* if to each excitation in the perturbed cell corresponds an excitation in the second cell, i.e. $\sigma_2/\sigma_1 = 1$.

(b) A dynamical régime that admits the propagation failure to occur at least once but not every time is called a *partial propagation failure*; σ_1, σ_2 satisfy $0 < \sigma_2/\sigma_1 < 1$.

(c) Dynamics with $\sigma_2/\sigma_1 = 0$ is called a *complete propagation failure*.

This classification holds for periodic as well as non-periodic dynamics. Even though the former dominated in the experiments, the latter did occur. A particular periodic firing sequence as indicated by the Pt electrodes in both cells is shown in figure 5. The firing vector is $(1, \frac{1}{2})$; the overall period is $2T$, i.e. $q = 2$. So the first cell is $\frac{1}{1}$ frequency-locked with the driving sequence of perturbations but $\frac{2}{2}$ phase-locked; the second cell is $\frac{1}{2}$ phase-locked with the external driving sequence. This dynamical régime is classified as a partial propagation failure. In fact, this is a nearly marginal case close to a transition to dynamics with $(\sigma_1, \sigma_2) = (1, 1)$.

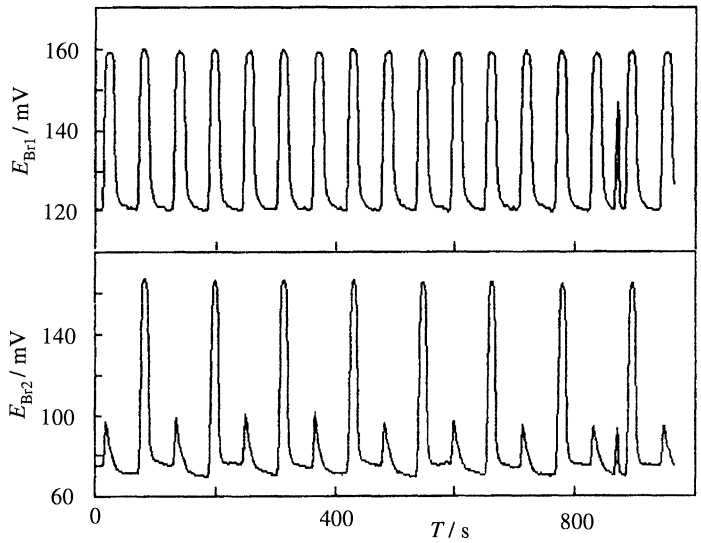

Figure 5. Time records of the measured potentials E_{Br1}, E_{Br2} of the bromide electrodes in the two cells; first cell was stimulated with the period $T = 58$ s; the amplitude $A \equiv c(Ag^+) = 9.5 \times 10^{-5}$ mol dm^{-3}; $z = 10$ mm; the firing vector (σ_1, σ_2) is equal to $(1, \frac{1}{2})$.

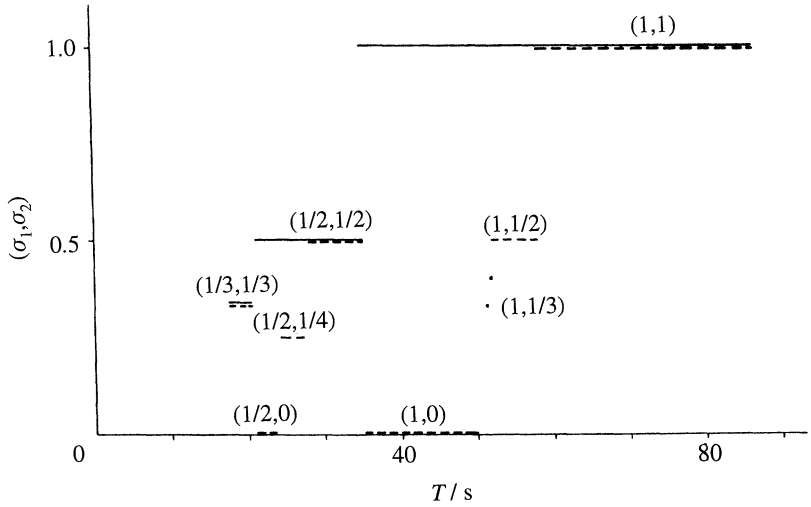

Figure 6. The plot of (σ_1, σ_2) against T constructed from experiments; $z = 10$ mm, $A \equiv c(Ag^+) = 7.5 \times 10^{-5}$ mol dm^{-3}. ——, First (externally driven) cell; - - -, second cell.

A plot of the firing number (or vector) against the period of stimulation and/or other control parameter(s) is called an 'excitation diagram' (Dolník *et al.* 1989; Finkeová *et al.* 1990; Takahashi *et al.* 1990). The plot of (σ_1, σ_2) against T is shown in figure 6; the firing vectors $(1, 1)$, $(1, \frac{1}{2})$, $(1, \frac{1}{3})$, $(1, 0)$, $(\frac{1}{2}, \frac{1}{2})$, $(\frac{1}{2}, \frac{1}{4})$, $(\frac{1}{2}, 0)$ and $(\frac{1}{3}, \frac{1}{3})$, all corresponding to periodic régimes, can be clearly identified from experiments. Non-periodic régimes do occur near the edges of main resonance regions but these are left out from the diagram. Experiments at high values of z reveal that when the cells are strongly coupled, the complex structure of the excitation diagram due to the propagation failure phenomenon is no longer present

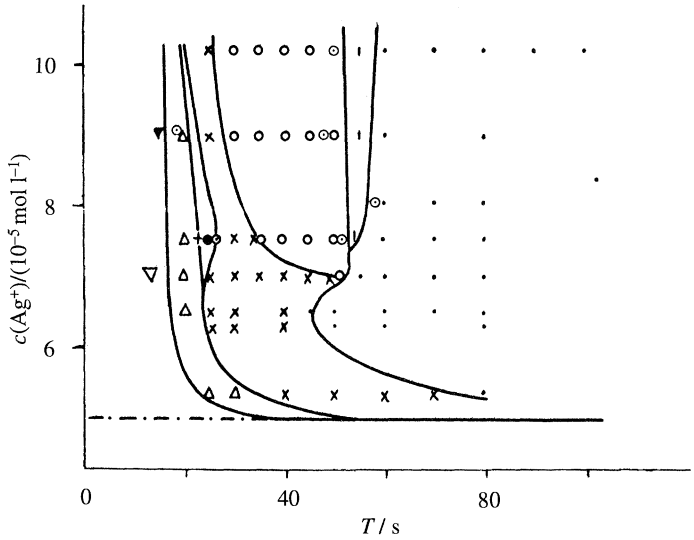

Figure 7. Period–amplitude excitation diagram constructed from experiments; the value of the firing vector (σ_1, σ_2) defines a partition of the parameter plane into regions with particular dynamic modes; coupling strength $z = 10$ mm. ·, $(1,1)$; |, $(1,\frac{1}{2})$; ○, $(1,0)$; ×, $(\frac{1}{2},\frac{1}{2})$; ●, $(\frac{1}{2},\frac{1}{4})$; +, $(\frac{1}{2},0)$; △, $(\frac{1}{3},\frac{1}{3})$; ▼, $(\frac{1}{4},\frac{1}{4})$; ▽, $(\frac{1}{4},0)$; ⊙, non-periodic.

and only complete propagation remains. A two-parameter excitation diagram in figure 7 is a projection of the firing vector into the A–T plane; the boundaries delineate regions of constant firing vectors. The diagram shows that a propagation failure may occur only if A is larger than about 7×10^{-5} mol dm^{-3} – a value well above the threshold at $A \approx 5 \times 10^{-5}$ mol dm^{-3}. Thus for slightly superthreshold amplitudes complete propagation prevails whereas a propagation failure becomes dominant as A is increased.

(*b*) *Phase model from BZ kinetics*

The kinetics of the BZ reaction has been thoroughly studied and its mechanism is fairly well known (Field & Burger 1985). There are many particular models of the BZ kinetics most of them derived from the Field–Körös–Noyes mechanism (Field, Körös & Noyes 1972); notably the Oregonator model (Field & Noyes 1974). Here we adopt a four-variable version of a recently improved Oregonator-like model (Zhabotinsky *et al.* 1993) – a simple but still reasonable model of the BZ mechanism.

A single CSTR with the BZ reaction is described by the evolution equations (2.1) with N=1. The concentrations x, y, u, z of the four species $HBrO_2$, Br^-, $HBrO_2^+$, Ce^{4+} constitute the components of $\boldsymbol{x}$ and the function $\boldsymbol{f}(\boldsymbol{x})$ is given by

$$\left.\begin{aligned} f_1 &= -r_1 + r_{-1} + r_3 - r_{-3} - 2r_4 - r_5 + r_7 - k_0 x, \\ f_2 &= -r_5 - r_7 + q r_8 + r_{13} + k_0(y_0 - y), \\ f_3 &= 2(r_1 - r_{-1}) - r_3 + r_{-3} - k_0 u, \\ f_4 &= r_3 - r_{-3} - r_8 + k_0(z_0 - z), \end{aligned}\right\} \tag{3.1}$$

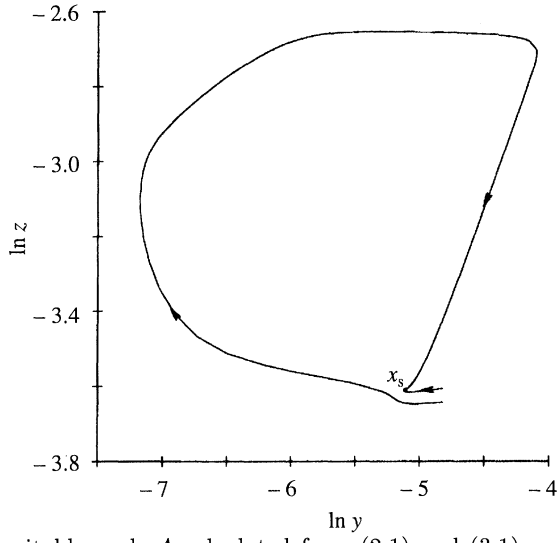

Figure 8. The excitable cycle Λ calculated from (2.1) and (3.1) and projected to the $\ln y$–$\ln z$ plane; parameter values are given in text. Λ is formed by two trajectories meeting at the steady state x_s, no other steady states are present.

where the reaction rates are

$$\left.\begin{aligned} r_1 &= k_1 h_0 A x, & r_{-1} &= k_{-1} u^2, & r_3 &= k_3 u(z_0 - z), \\ r_{-3} &= k_{-3} x z, & r_4 &= k_4 x^2, & r_5 &= k_5 h_0 x y, \\ r_7 &= k_7 h_0 A y, & r_8 &= k_8 B z, & r_{13} &= k_{13} B. \end{aligned}\right\}$$

Here the k_is are the reaction rate coefficients, h_0 is Hammet acidity function, k_0 is the volumetric flow rate divided by the volume of the reactor, y_0, z_0 are inlet concentrations and q is a stoichiometric factor. The concentrations $A = [\mathrm{BrO_3^-}]$, $B = [\mathrm{CHBr(COOH)_2}]$ are assumed in excess and therefore constant. The values of the rate coefficients are taken from (Field & Försterling 1986), other parameters are set to values corresponding to the experiments: $A = 0.3$ mol dm^{-3}, $B = 0.1$ mol dm^{-3}, $h_0 = 0.82$ mol dm^{-3}, $z_0 = 0.006$ mol dm^{-3}, $y_0 = 0.01$ mol dm^{-3}, $q = 1$. Under these conditions the dynamics in an isolated cell undergoes a Hopf bifurcation for $k_0^* \approx 1.2 \times 10^{-4}$ s^{-1}. The system is excitable in a range of the flowrates just above k_0^* in a good agreement with the value of 5.4×10^{-4} s^{-1} used in the experiments.

The model provides an excitable cycle Λ with one stationary state, i.e. Λ is not a closed curve, see figure 8. Now we want to use Λ for deriving a map analogous to that obtained from the simple phase model (2.2) and (2.3). One way would be to mechanically follow the approach from § 2, find a velocity function $v(\phi)$ on Λ and integrate the (2.2) and (2.3). However, the way (2.2) and (2.3) are perturbed does not correspond well to the addition of silver ions in experiments (Finkeová *et al.* 1990). Rather we retain only the essential features of (2.6) and (2.7) and use the idea of the 'finite-time-jump map' and effective amplitudes as implied by (2.10) and (2.11). A conjectured form of a phase mapping $\Pi(\phi_1, \phi_2)$ between the kth and the $(k+1)$st pulses for two coupled BZ excitators T-periodically

perturbed by adding A silver ions is

$$\phi_{1,k+1} = g(\phi_{1,k}; \varepsilon_1, \tau) + D(d,\tau)(g(\phi_{2,k}; \varepsilon_2, \tau) - g(\phi_{1,k}; \varepsilon_1, \tau)), \tag{3.2}$$

$$\phi_{2,k+1} = g(\phi_{2,k}; \varepsilon_2, \tau) + D(d,\tau)(g(\phi_{1,k}; \varepsilon_1, \tau) - g(\phi_{2,k}; \varepsilon_2, \tau)), \tag{3.3}$$

where $\varepsilon_1 = A(1 - D_{\mathrm{in}})$, $\varepsilon_2 = AD_{\mathrm{in}}$, $D_{\mathrm{in}} = \frac{1}{2}(1 - \mathrm{e}^{-2d\tau_{\mathrm{in}}})$, $D = \frac{1}{2}(1 - \mathrm{e}^{-2d\tau})$, $T = \tau_{\mathrm{in}} + \tau$; τ_{in} is a short initial time interval. The function $g(\phi; \varepsilon, T)$ describes the dynamics of an isolated cell T-periodically perturbed by Ag^+ pulses of amplitude ε which must be empirically derived from the BZ model.

The equations (3.1) do not include silver ions as an independent variable. However, Ag^+ acts by removing Br^- via a fast equilibrium reaction $\mathrm{Ag}^+ + \mathrm{Br}^- \rightleftharpoons \mathrm{AgBr}$; considering the solubility product s of this reaction, the amount of Br^- removed within the pulse is (Dolník *et al.* 1989)

$$\delta y = \tfrac{1}{2}(s/y + \varepsilon + y - [(s/y + \varepsilon - y)^2 + 4s]^{1/2}).$$

The map g is constructed numerically by taking many points on Λ, subtracting δy from the current value of $y \equiv [\mathrm{Br}^-]$ and integrating (2.1) and (3.1) from 0 to T. The perturbation relaxes back to the excitable cycle Λ within a short time (< 1 s) and after choosing a parametrization by ϕ on Λ (we took the arclength in the $(\ln x, \ln y, \ln u, \ln z)$-space) g is obtained. We used a combination of hyperbolic tangents to cast $g(\phi; \varepsilon, T)$ into an analytic form. The graph of g within the range of T and A used in experiments is shown in figures 9 and 10. There is a steep but continuous portion of the graph rather than a discontinuity since we have not made the approximation of 'cutting off' the threshold set; on the other hand g is a mapping of an interval rather than of a circle. The location of the drop is independent of T (cf. figure 9) and is shifted to the left with increasing A (cf. figure 10). This is in agreement with the analogous mapping (2.8) of the abstract phase model. The details of the dynamics of iterated g will be discussed elsewhere, our aim here is to understand the essential features of the dynamics of the map $\Pi(\phi_1, \phi_2)$ defined by the coupled system (3.2) and (3.3).

As in § 2, a sudden drop of $g(\phi; \varepsilon_i; T)$ defines a phase of marginal refractoriness ϕ_{ir} in the ith cell. Thus when iterating $\Pi(\phi_1, \phi_2)$ a firing in the ith cell results every time $\phi_{i,k} > \phi_{ir}$. Consequently the firing vector (ν_1, ν_2) can be calculated. Even though approximate, the mapping $\Pi(\phi_1, \phi_2)$ reproduces salient features of the experiments. When d is small, transitions from complete propagation to partial and ultimately complete propagation failure occur repeatedly as T is decreased, see figure 11. An interesting observation is made for medium and large T; then D is near to $\frac{1}{2}$ and hence the phases in both cells just before the pulse are nearly the same. Since $\phi_{1r} < \phi_{2r}$, the perturbation at phases $\phi_1 \approx \phi_2$ results in an excitation event in the first cell but fails to initiate a firing in the second one if $\phi_{1r} < \phi_1 < \phi_{2r}$. Thus although the dynamics of the phase map suggest a near to perfect synchronization at the end of the relaxation phase, the immediate response to perturbation may dramatically differ in both cells. Numerical calculations also show that when d is large, only complete propagation is possible. Further refinements of Π are deemable.

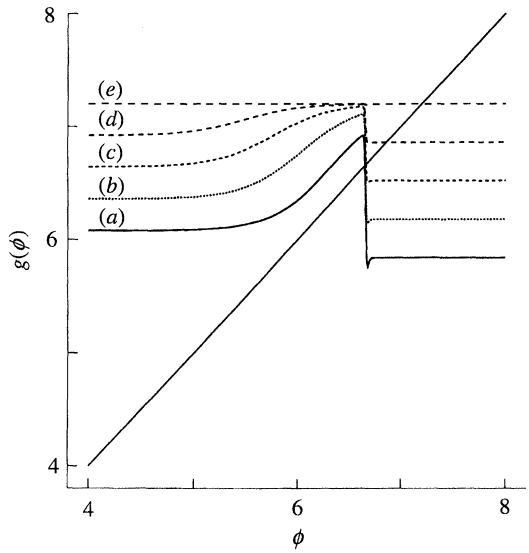

Figure 9. The phase excitation map $g(\phi)$ for an isolated CSTR with the BZ reaction periodically perturbed by injections of Ag^+ ions; $A = 1.0 \times 10^{-4}$ mol dm^{-3}; the curves (a)–(e) correspond to $T = 20, 40, 60, 80, 100$ s respectively; see text for other parameter values.

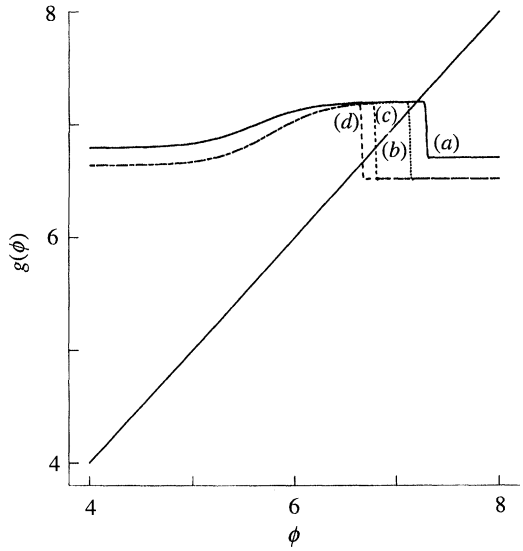

Figure 10. The phase excitation map $g(\phi)$ for an isolated CSTR with the BZ reaction periodically perturbed by injections of Ag^+ ions; $T = 60$ s; the curves (a)–(d) correspond to $A = 0, 1.0\times10^{-6}$, 1.0×10^{-5}, 1.0×10^{-4} mol dm^{-3} respectively; see text for other parameter values.

4. Discussion and conclusions

The excitation diagrams presented in figures 1, 2, 6, 7 and 11 all possess the same features – the most prominent being the repeated transitions from complete propagation to complete failure of propagation as the forcing period is decreased. This is true even for the abstract phase model discussed in § 2 and points to a generic occurrence of the propagation failure phenomenon. The reason for this

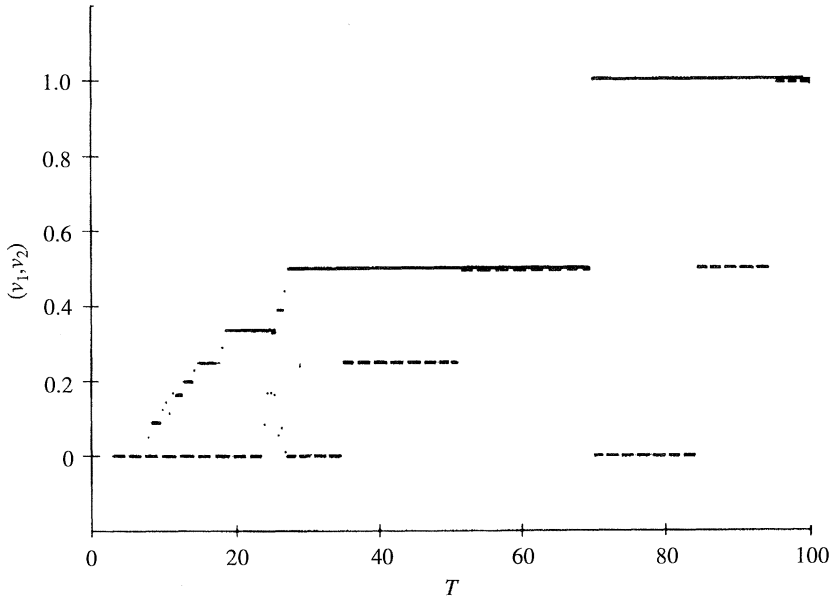

Figure 11. The plot of the firing vector against T for the BZ phase mapping (3.2), (3.3); $A = 1.0 \times 10^{-4}$ mol dm^{-3}, $d = 0.01$, $\tau_{\text{in}} = 1.5$ s; ——, first (externally driven) cell; - - -, second cell.

striking agreement follows from the T-dependence of the integral diffusion coefficient D and the dynamics of the 'finite-time-jump' map (2.10) and (2.11). Equation (2.11) implies that the phase of marginal refractoriness in the second cell is larger than that in the first cell. Consequently for T sufficiently large D approaches its upper limit of $\frac{1}{2}$ and the phases in both cells tend to be almost the same. The different ability of both cells to fire then directly results in repeated cascades as indicated by the excitation diagrams.

Construction of models for networks of excitable units with a more complex topology (linear and cyclic arrays, various planar structures) based on coupled phase excitation maps can proceed as a straightforward extension of the approach outlined here. Remarkable agreement between the excitation diagrams constructed from experiments on one hand and the diagrams calculated from two simple phase models on the other, gives support to further development of the method and opens wide possibilities of applications to biochemical and biological systems; for example those directly involved in signal transmission through synapses, such as the acetylcholine system. Once the phase map for a particular dynamics of an excitable unit has been constructed (either directly from experiments or from a detailed physico-chemical model), a model of a network is directly available. A detailed knowledge of the dynamics of such a coupled array would help to bridge the gap between the rather formal neural networks approach and the accumulating experimental knowledge about functioning of particular neurophysiological systems (Steriade *et al.* 1993; Lebender *et al.* 1993).

References

Alexander, J. C., Doedel E. J. & Othmer, H. G. 1990 On the resonance structure in a forced excitable system. *Siam. J. appl. Math.* **50**, 1373–1418.

Barkley, D. 1991 A model for fast computer simulation of waves in excitable media. *Physica* D **49**, 61–70.

Chawanya, T., Aoyagi, T., Nishikawa, I., Okuda, K. & Kuramoto, Y. 1993 A model for feature linking via collective oscillations in the primary visual cortex. *Biol. Cybern.* **68**, 483–490.

Dolník, M., Schreiber, I. & Marek, M. 1986 Dynamic régimes in a periodically forced reaction cell with oscillatory chemical reaction. *Physica* D **21**, 78.

Dolník, M., Finkeová, J., Schreiber, I. & Marek, M. 1989 Dynamics of forced excitable and oscillatory chemical reaction systems. *J. phys. Chem.* **93**, 2764.

Dolník, M. & Marek, M. 1991 Phase excitation curves in the model of forced excitable reaction system. *J. phys. Chem.* **95**, 7267.

Dolník, M., Marek, M. & Epstein, I. 1992 Resonances in periodically forced excitable systems. *J. phys. Chem.* **99**, 3218.

Field, R. J., Körös, E. & Noyes, R. M. 1972 Oscillations in chemical systems. II. Thorough analysis of temporal oscillation in the bromate-cerium-malonic acid system. *J. Am. chem. Soc.* **94**, 8649–8664.

Field, R. J. & Noyes, R. M. 1974 Oscillations in chemical systems IV. Limit cycle behavior in a model of a real chemical reaction. *J. chem. Phys.* **60**, 1877.

Field, R. J. & Försterling, H.–D. 1986 On the oxybromine chemistry rate constants with cerium ions in the Field–Körös–Noyes mechanism of the Belousov–Zhabotinskii reaction: the equilibrium $HBrO_2 + BrO_3^- - + H^+ \rightleftharpoons 2BrO_2 + H_2O$. *J. phys. Chem.* **90**, 5400–5407.

Field, R. J. & Burger, M. (eds) 1985 *Oscillations and traveling waves in chemical systems.* New York: Wiley.

Finkeová, J., Dolník, M., Hrudka, B. & Marek, M. 1990 Excitable chemical reaction systems in a CSTR. *J. phys. Chem.* **94**, 4100.

Fujita, I., Tanaka, K., Ito, M. & Cheng, K. 1992 Columns for visual features of objects in monkey inferotemporal cortex. *Nature, Lond.* **360**, 343–346.

Glass, L. & Mackey, M. C. 1988 *From clocks to chaos. The rhythms of life.* Princeton University Press.

Glass, L., Hunter, P. & McCulloch, A. 1991 *Theory of heart.* New York: Springer Verlag.

Hammer, M. 1993 An identified neuron mediates the unconditioned stimulus in associative olfactory learning in honeybees. *Nature, Lond.* **366**, 59–63.

Holden, A. V., Markus, M. & Othmer, H. G. (eds) 1991 *Nonlinear wave processes in excitable media.* New York: Plenum Press.

Kaneko, K. 1990 Simulating physics with coupled map lattices. In *Formation, dynamics and statistics of patterns* (ed. K. Kawasaki, M. Suzuki & A. Onuki), vol. 1. Singapore: World Scientific.

Kondo, T., Strayer, C. A., Kulkarni, R. D., Taylor, W., Ishiura, M., Golden, S. S. & Johnson, C. A. 1993 Circadian rhythms in prokaryotes: Luciferase as a reporter of circadian gene expression in cyanobacteria. *Proc. natn. Acad. Sci. U.S.A.* **90**, 5672–5676.

Kosek, J. & Marek, M. 1993 Coupled excitable cells. *J. phys. Chem.* **97**, 120–127.

Kuramoto, I. 1991 Collective synchronization of pulse-coupled oscillators and excitable units. *Physica* D **50**, 15–30.

Lebender, L., Schneider, F. W., Friedrich, M. & Marek, M. 1993 Neural net predicting devil's staircase of spikes and bursts. In *Proc. Conf. Computer Simulation in Biology, Ecology and Medicine.* Copenhagen.

Marek, M. & Schreiber, I. 1991 *Chaotic behaviour of deterministic dissipative systems*, ch. 5. Cambridge University Press.

Okamoto, M. 1992 Biochemical switching device: biomimetic approach and application to neural network study. *J. Biotechnol.* **24**, 109–127.

Schreiber, I. & Marek, M. 1993 Chaos in forced and coupled chemical oscillators and excitators. In *Chaos in chemical and biological systems* (ed. R. J. Field & Z. Györgyi). Singapore: World Scientific.

PHILOSOPHICAL TRANSACTIONS OF THE ROYAL SOCIETY A MATHEMATICAL, PHYSICAL & ENGINEERING SCIENCES

Steriade, M., McCormick, D. A. & Sejnowski, T. J. 1993 Oscillations in the sleeping and aroused brain. *Science, Wash.* **262**, 679–685.

Stuchl, I. & Marek, M. 1982 Dissipative structures in coupled cells: experiments. *J. chem. Phys.* **77**, 2956.

Takahashi, N., Hanyu, Y., Musha, T., Kubo, R. & Matsumoto, G. 1990 Global bifurcation structure in periodically stimulated giant axons of squid. *Physica* D **43**, 318–334.

Tanaka, K. 1992 Inferotemporal cortex and higher visual functions. *Current Opinion Neurobiology* **2**, 502–505.

Winfree, A. T. 1977 *When time breaks down.* Princeton University Press.

Yoshimoto, M., Yoshikawa, K. & Mori, Y. 1993 Coupling among three chemical oscillators: synchronization, phase death and frustration. *Phys. Rev.* **47**, 864–874.

Zeyer, K. P., Holz, R. & Schneider, F. W. 1993 Continuous coupling of chaotic and periodic states of chemical oscillators with and without time delay. *Ber. BunsenGes. phys. Chem.* **97**, 1112–1119.

Zhabotinsky, A. M., Buchholz, F., Kiyatkin, A. B. & Epstein, I. 1993 Oscillations and waves in metal-ion-catalyzed bromate oscillating reactions in highly oxidized states. *J. phys. Chem.* **97**, 7578–7584.

PHILOSOPHICAL TRANSACTIONS OF THE ROYAL SOCIETY A MATHEMATICAL, PHYSICAL & ENGINEERING SCIENCES